Eur. J. Mineral.
2004, **16**, 585–595

A microstructural study of a "crack-seal" type serpentine vein using SEM and TEM techniques

MURIEL ANDREANI*[1], ALAIN BARONNET**, ANNE-MARIE BOULLIER* and JEAN-PIERRE GRATIER*

* LGIT, Université Joseph Fourier, BP 53, 38041 Grenoble cedex 9, France
[1] Corresponding author, e-mail: Muriel.Andreani@obs.ujf-grenoble.fr
** CRMC2-CNRS, Campus Luminy, case 913, 13288 Marseille Cedex 9, France

Abstract: Serpentine banded veins are frequently observed in massive serpentinized peridotites. They form by extension or extensional shearing during hydrothermal alteration of peridotites. Serpentine minerals display different structural varieties, the occurrences of which are not well defined in terms of temperature, pressure, and chemistry, but may be controlled by departure from equilibrium and by the local water/rock ratio. Serpentines are therefore potential markers of environmental conditions during vein formation. However, they have never been used to assess the mechanism of banded vein formation. Using multi-scale microscopy techniques, and comparing detailed observations of natural samples from cm to nm scale with available experimental results, we attempt to deduce constraints on growth mechanisms of serpentines in banded veins. The banded internal structure and the filling along the vein-wall contact suggest a crack-seal mechanism of formation. Each crack is homogeneously filled with chrysotile and some rare polygonal serpentines (tubular serpentine varieties) and disseminated patches of gel-type protoserpentine. The tubes are not parallel to each other, but clearly show a preferred orientation perpendicular to the crack wall. Recent synthesis experiments describe a temporal succession of occurrence of these three serpentine microstructures. The observations suggest that such an evolution can occur in natural samples. The geometric peculiarities of macroscopic growth mechanisms in microscopic interstices may account for capillary effects. Based on this consideration, a simple qualitative model of serpentine banded vein formation is proposed. This model provides a possible origin for the enhancement and maintenance of a diffusional mass transfer from the matrix to the crack. This model also predicts the very good tracking of vein opening directions in such veins.

Key-words: serpentine, microstructures, crack-seal, growth, TEM.

1. Introduction

The study of veins in deformed rocks is of particular interest because they are markers of rock deformation history, mass transfer processes, and also a site of mineral crystallization. They can provide reliable information if their formation mechanism is well understood. Factors concerning vein formation that need to be addressed include i) cause of opening and propagation, ii) transport mechanism and iii) precipitation conditions of the vein filling material. They can all vary widely and the internal microstructure of veins carries an inprint of formation conditions. These processes are still being discussed, in particular for banded veins, and are usually explained by the crack-seal mechanism. Crack-seal is a mechanism proposed to explain the formation of veins showing banding, made for example by wall or fluid inclusions. This model consists in an incremental opening followed by complete sealing (Ramsay, 1980) of small successive cracks. Hundreds of cracking episodes are commonly interpreted this way. Episodic crack openings have been explained by oscillations in fluid pressure or bulk stress (Ramsay, 1980) and more recently by a crystallization pressure (Wiltschko & Morse, 2001). However, this mechanism is not linked to a specific transport mechanism or cause for precipitation. Transport of elements may occur by fluid advection or/and by local diffusion within the pore-fluid (Fischer & Brantley, 1992). Crystal shape within the veins can be stretched or elongate-blocky (Fisher & Brantley, 1992) and authors still discuss whether or not the fibrous texture can be attributed to the crack-seal mechanism (Cox & Etheridge, 1983; Urai *et al*., 1991; Bons & Jessel, 1997; Means & Li, 2001). The cause of material precipitation in veins is due to a variation of the chemical activity of the solute that can be attributed to changes in temperature, fluid pressure, differential stress...

The majority of the previous studies concerned quartz or calcite veins in low-grade metamorphism environments with high fluid pressure. Although serpentine banded veins are frequently observed in massive serpentinized peridotites (Wicks & Whittaker, 1977; Dilek *et al.*, 1997), no detailed observations of their internal microstructure have been made. Serpentine minerals display four main structural varieties: lizardite (plate-like structure), chrysotile (cylindrical structure), polygonal serpentine (tubular type with a poly-

0935-1221/04/0016-0585 $ 4.95
DOI: 10.1127/0935-1221/2004/0016-0585

gonized section) and antigorite (modulated structure). For all but antigorite, recent experiments showed that their occurrence may also be controlled by departure from equilibrium and by the local water/rock ratio (Grauby *et al.*, 1998; Normand *et al.*, 2002). Therefore, serpentines are potential markers of specific environmental conditions during vein formation. This possibility was therefore explored by comparing detailed observations of natural samples with available experimental results in order to indicate the constraints on growth mechanisms of serpentines in veins and to obtain a better understanding of the formation processes of banded veins in general.

2. Geological setting and sample location

2.1. Geological setting

The subduction of the Pacific plate under the North America margin from late Jurassic to late Cenozoic resulted in the formation of the Franciscan accretionary complex along the western coast of North America (Bailey *et al.*, 1964; Atwater, 1989). In California, this complex is a mixing of deformed and variably metamorphosed sedimentary rocks and oceanic crustal and mantle components. Their subduction to 10 to 30 km depth resulted in metamorphism under HP-LT conditions before they were brought back to the surface (Ernst, 1971; Page, 1981).

2.2. Serpentinite samples

Partially to totally serpentinized peridotite bodies are distributed throughout the Franciscan melange (Page, 1972; Page *et al.,* 1998; Coleman, 2000). Samples of serpentinites have been collected north of Santa Barbara, California (Fig. 1a), along the Santa Ynez Fault, in the Blue Canyon, where this 130 km long fault cuts across an elongated serpentinite body (1 x 0.1 km). The structures related to the Santa Ynez Fault are strictly limited to a narrow fault gouge. Surrounding massive serpentinites are organized in decimetric to metric blocks that are not affected by the recent San Andreas faulting. Thus, we can access to markers of the serpentinite history before active faulting. Block surfaces show striations and blue-green sliken-fibres which suggest that they have undergone rigid rotation by sliding past one another on their surfaces during their complex history (Twiss & Gefell, 1990).

Serpentinized peridotites show the pseudomorphic mesh and bastite replacement textures of olivine and pyroxene respectively (Wicks & Whittaker, 1977) with some rare relicts and these textures are typical of oceanic hydration. Several generations of veins are also observed, comparable to those described by Dilek *et al.* (1997) or Stamoudi (2002) in serpentinized peridotites exposed on the seafloor of the Mid-Atlantic Ridge (MARK area) and the East-Pacific Ridge (Hess-Deep). Thus, they could form during oceanic hydrothermal history of the past Pacific oceanic crust. A 3D-network of planar blue-

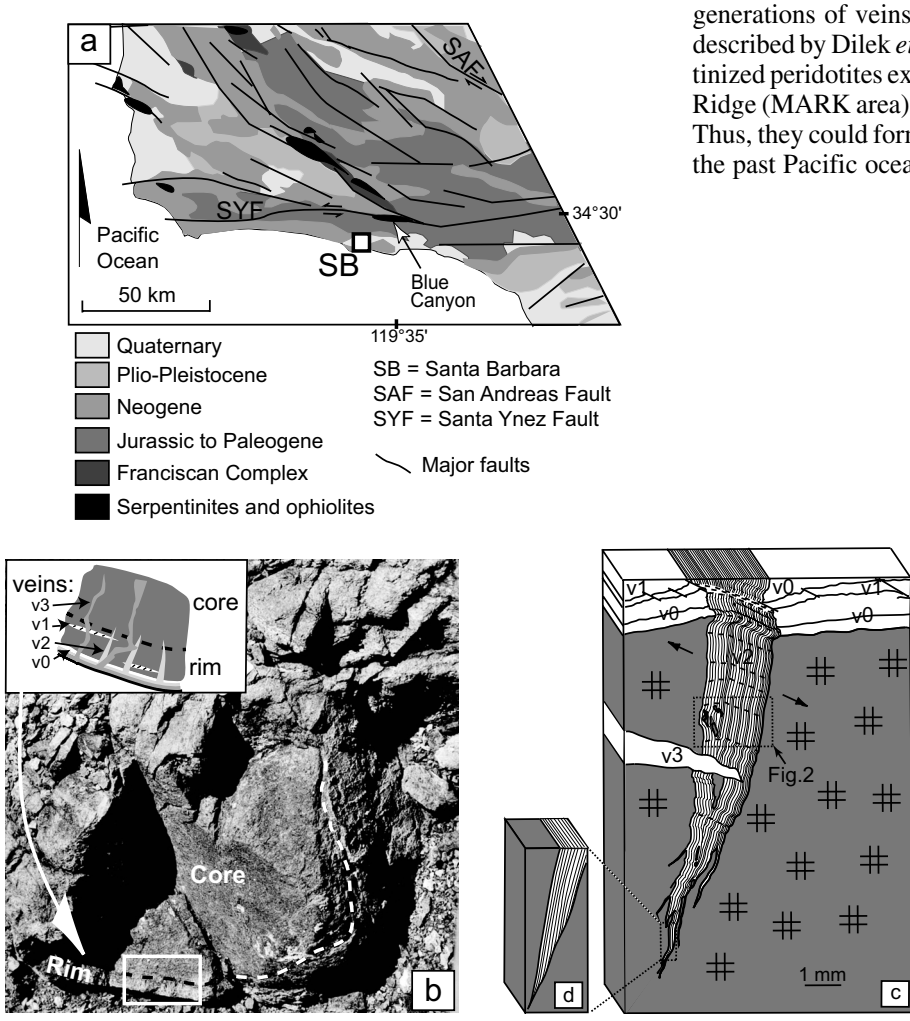

Fig. 1. Location and structural sketch of the studied vein. a: Geological map of California, north of Santa Barbara (S.B.) and the major faults of the San Andreas system. Massive serpentinized peridotites are adjacent to the Santa Ynez Fault (S.Y.F.), along the Blue Canyon. b: Picture of a massive serpentinized peridotite block at the outcrop. A schematic close-up of the different generations of veins is drawn on the upper-left corner. The chronological order of the veins is as follows: v0 & v1: primary serpentine veins, v1 is a fibrous vein; v2: banded serpentine vein; v3: later isotropic serpentine vein. c: Structural diagram of the banded vein (v2) developing perpendicular to the block surface. The double cross pattern represents the serpentinized peridotite matrix. Dotted lines accross v2 follow optical "trails". d: Geometry of the vein tip. This indicates that increments are preferentially younger from the right to the left.

banded veins is developed both along and normal (in two perpendicular directions) to the block limits (Fig. 1b). The diagram in Fig. 1c presents the geometry and structure of a vein in a plane perpendicular to the vein walls. This vein crosscuts a massive serpentinite block and has been studied in detail. Vein width varies from few μm to several mm. This type of vein has been interpreted as the result of incremental stress release during unroofing of serpentinized peridotite in the case of the MARK area (Dilek *et al.*, 1997). This is in good agreement with our observations which indicate a syntectonic vein formation in extension and/or extensional shearing, that accommodates progressive separation and rotation of relatively undeformed neighbouring serpentinite blocks (Fig. 1b). Nevertheless, the relative 3D-radial geometry of massive serpentinized blocks and vein arrays suggests that these fractures could also accommodate a volume increase of the peridotite during its hydration to serpentinite, as suggested by O'Hanley (1992).

3. Microscale observations of the banded internal fabric of the vein

3.1. Optical microscopy: vein texture and morphology

A segment of the vein is pictured on Fig. 2a and 2b. The internal structure is revealed only under crossed polars. This type of vein has a variable birefringence that can reach abnormal 2nd order colours for a thin section of 30 μm thickness. Two types of structure, similar to those described as bands and trails by Ramsay (1980), can be observed. They are drawn on Fig. 1c. First, a finely spaced banding is observed parallel to vein margins. The bands are separated by lines of low birefringence and their irregular shape perfectly mimics the shape of the vein margins that can be superimposed on each other (Fig. 2a). The geometry of the margins are thus preserved across the vein width, except when wall fragments have been included in the vein filling (Fig. 2b). Secondly, the simultaneous extinction of zones perpendicular to the banding defines the trails which link edge irregularities across the vein width (Fig. 2a). No inclusions or second phases are observed within these trails so they are only extinction figures. The minimal width of one band is close to 1 μm and the maximum observed is less than 5 μm. Statistical analysis reveals a characteristic width of 3 μm and a random succession of band widths (Renard *et al.*, in press).

Crack propagation is not guided by matrix texture except when cutting through bastites where it preferentially follows the primary {110} cleavage planes of pyroxene. At grain-scale (hundreds of nm), lizardite being the main mesh component, the opening path might be locally guided or at least helped by the weak (001) plane of lizardite. The internal structure of the vein is often asymmetric close to the tip, as drawn on the simplified scheme of the tip on Fig. 1c. Bands tend to be discordant on the right vein margin and concordant with the left one.

The grain size of serpentine crystals is usually submicronic and cannot be observed with a petrographic microscope, so electron microscopy is needed to identify the serpentine type and to understand the features seen in optical microscopy.

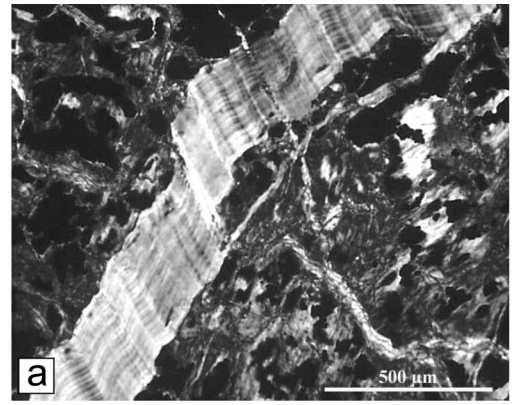

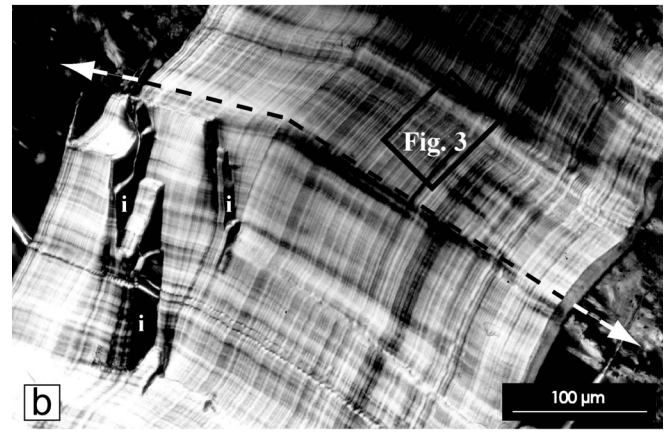

Fig. 2. Serpentine banded veins observed under crossed polars. a: This low magnification image of a vein shows that the bands are parallel to the walls and perfectly mimics their morphology. The margins can be superimposed on each other and linked by the trails. b: Enlargement of Fig. 1c. Bands are parallel to the NE-SW axis of the picture and trails are underlined by the dotted line. i: wall rock inclusions.

3.2. SEM: organisation of vein filling in space

Scanning Electron Microscopy (SEM) gives the geometry of vein filling at an intermediate scale between micrometric (thin section) and nanometric (TEM) scales.

The massive sample containing the banded vein described above was broken perpendicularly to the vein, cleaned in an ultrasonic bath, then glued on a support and covered with a 10-15 nm thick carbon coating. SEM imaging was performed on a JEOL 6320FEG scanning electron microscope at the CRMC2 (CNRS, Marseille, France).

At low magnification (Fig. 3a), individual bands are already visible. Smallest units range from 1 to 4 μm in thickness. Each band shows the same internal structure: a homogeneous filling of tubular-shaped serpentine crystals with a preferred orientation perpendicular to banding (Fig. 3b and 3c). Successive bands are separated by a plane marked by the termination of serpentine tubes, along which fracturing due to sample preparation is localized. Locally, they appear to be embedded in a poorly crystallized phase (Fig. 3c). De-

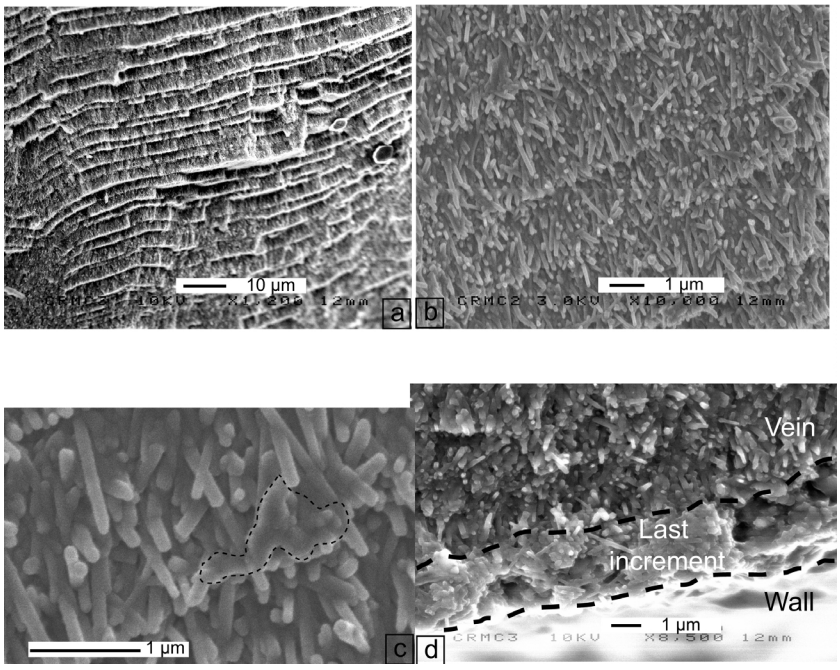

Fig. 3. a: Low magnification SEM image of vein filling (area indicated in Fig. 2b). Note the irregular thickness of bands ranging from 5 µm to less than 1 µm. b, c: Enlargement on bands. Tube diameters are around 100 nm and a residual porosity exists between them. Within one band, the tubes seem to be locally glued in a shapeless, poorly crystallized phase (P1: circled). d: Image of the vein-wall contact. It is marked by a layer filled with a tubular serpentine and a poorly crystallized phase.

spite the high density of tubes, a residual porosity remains between them. Unfortunately, owing to the sample geometry, it is not possible to measure the tube length, nor to check whether one tube necessarily spans a whole band. The vein-wall interface has also been investigated (Fig. 3d). Along the left wall of the vein on Fig. 1c and 1d (the youngest increment), a µm-size interstice is filled with the "gel-type" (poorly crystallized) phase in which very small tubular-shaped crystals can be distinguished. Round and smooth pores within this material may be interpreted as primary porosity. This layer at the vein-wall interface could represent the last addition of a new band, thus defining an antitaxial vein filling.

Only TEM observations can allow a rigorous identification of serpentine microstructures in this vein and specify their mutual arrangements.

3.3. TEM: identification of serpentine microstructures and their intergrowths

TEM images were taken with a JEOL 2000fx high-resolution transmission electron microscope at the CRMC2 (CNRS, Marseille, France), with a 200kV accelerating voltage. A thin section, attached with Lakeside® resin to the glass substrate, was cut perpendicular to the banded vein. A single-hole copper TEM grid was glued on a selected area of the section. The specimen was extracted from the thin section by heating the resin after drilling around the grid. Prior to observation, specimens were thinned by ion-beam milling (Precision Ion Polishing System – Gatan 690) and carbon-coated.

The banding direction was determined under a petrographic microscope before TEM observation. Banding is not as evident as on SEM images, probably because of the milling which can result in a slightly inclined section compared to banding, and to an extremely reduced surface of observation (few µm) around the hole made by ion-beam milling. Nevertheless, images confirm the preferred orientation of tubes (Fig. 4b). It was also found that, on the same milled sample, areas with a majority of longitudinal sections (Fig. 4b) tend to alternate with zones containing longitudinal, oblique and cross-sections (Fig. 4a).

Two varieties of tubular serpentine minerals are identified (Fig. 5). Cylindrical tubes with the smallest diameter (< 100 nm) predominate and are chrysotile (P2 phase) (Baronnet & Devouard, 1996). The second type of tube is shorter and shows polygonized sections and a larger diameter (> 100 nm). This corresponds to polygonal serpentines (P3 phase) (Zuss-

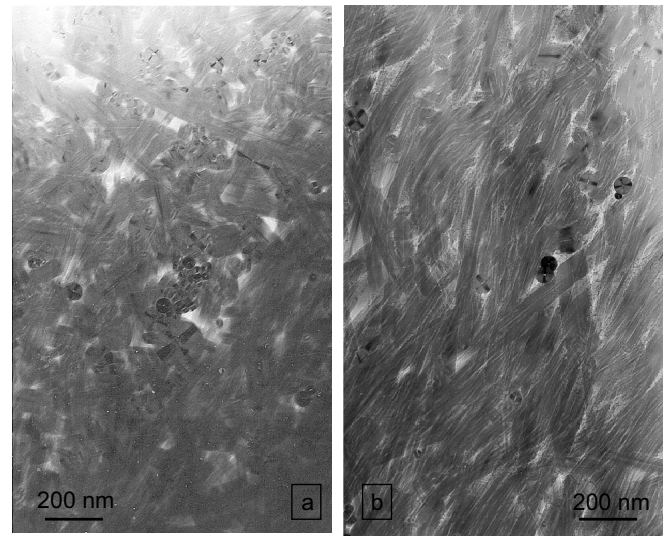

Fig. 4. TEM images of the vein-filling.An alternance of the two following microtextures is observed. a: TEM image of a zone with longitudinal, oblique and cross sections of chrysotile and polygonal serpentine. The lack of a preferred orientation of tubes should result in a low birefringence under crossed polars that can correspond to the limit between bands. b: TEM image of a zone with a majority of longitudinal sections. This should correspond to the part of the bands displaying a higher birefringence.

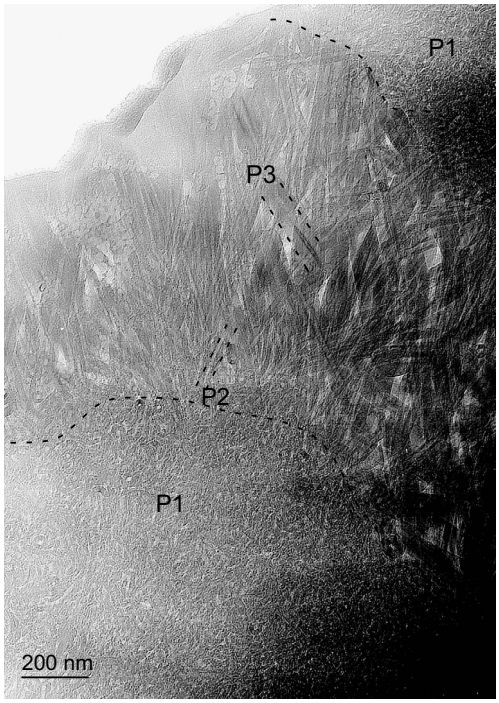

Fig. 5. TEM image of the vein-filling minerals. Three serpentine types can be identified: P1: protoserpentine – gel-type, poorly crystallized phase; P2: chrysotile – cylindrical structure with a diameter < 100 nm; P3: polygonal serpentine – tubular structure with a polygonized section and a diameter usually > 100 nm.

man *et al.*, 1957; Devouard *et al.*, 1997). A third serpentine phase is poorly crystallized (P1 phase): the protoserpentine. It has seldom been found in natural samples but has been observed in synthesis experiments (Grauby *et al.*, 1998). Fig. 5 illustrates a patch of protoserpentine from which small tubes seem to grow radially. Indeed, protoserpentine contains few nm-sized particles that seem to roll up.

4. Chemical composition

Serpentine minerals, except antigorite, are trioctahedral 1:1 sheet silicates represented by the ideal formula $Mg_3Si_2O_5(OH)_4$. The principal substitutions are $FeMg_{-1}$ and $(Al, Fe^{3+})^{VI}$ $(Al, Fe^{3+})^{IV}$ $Mg_{-1}{}^{VI}$ $Si_{-1}{}^{IV}$. Measurements were done in order to test for chemical variations: (i) between the vein and the host rock, (ii) across the vein (*e.g.* during vein formation) and (iii) within one band (between the different structural type).

4.1. Electron microprobe analysis (EMPA)

Analyses within the matrix and the vein were performed with a Cameca SX100 electron microprobe equipped with four wavelength-dispersive spectrometers (WDS) at the DSTU- Montpellier (France). Spot size (~3 µm) is similar to the mean band thickness, which does not allow comparison between successive bands, but by taking several measurements scattered across the vein it is possible to detect any large scale variations. Compositions are reported in oxide-weight % (wt%) along with the structural formulae in atom per formula unit (a.p.f.u.) calculated on the basis of seven oxygens (Table 1).

The chrysotile-polygonal serpentine vein cuts across a massive serpentinized peridotite matrix showing a pseudomorphic mesh and bastite texture. Mesh and bastite textures in serpentinized peridotites have been intensively investigated and lizardite is the dominant serpentine variety in the matrix, plus chrysotile and oxides (*e.g.* Coleman & Keith, 1971; Dungan, 1979; Viti & Mellini, 1998). The concentration of major cations (Mg, Si, total Fe, Al) is relatively constant in all samples with a general low amount of Al. Within the matrix, small variations in Ni and Cr contents are noted. They can be explained by the various nature of the precursor mineral. Indeed, preferential replacement of Mg by Ni and Cr may occur to a small extent in serpentine when it replaces olivine (mesh texture) and pyroxene (bastite), respectively (Dungan, 1979; Viti & Mellini, 1998). Cl and F are seldom detected but can appear locally, in very small amounts.

At EMPA scale, vein composition is highly homogeneous for all elements and is independent of distance from the edge. Ni and Cr contents are very low, close to the detection limit, as are Cl and F that appear locally.

4.2. Microanalysis of serpentine structural types

The sample prepared for TEM in section 3.3 (Fig. 5) was used again. The details of its preparation are explained in section 3.3. It contains the three different types of serpentine (protoserpentine, chrysotile and polygonal serpentine) encountered in the vein. Each serpentine type was analysed separately with a transmission electron microscope JEOL 2000fx equipped with a Tracor Northern 5520 X-ray energy dispersive system, working under a 200 kV accelerating voltage. Diameters of analysed surfaces are around 30 nm. Cliff-Lorimer K-factors $k_{i,Si}$ with i=Mg, Fe, Al, Cr, Ni, were calibrated against natural and synthetic standards. All the analyses were run on the same day. Serpentines are not very resistant under the electron beam, especially the less organized types of protoserpentine. This constraint has limited the number of analyses. Compositions in atom per formula unit (a.p.f.u.) are reported in Table 2.

Results are comparable to those obtained by electron microprobe. Small variations in composition can be noted within one type of serpentine but the mean compositions of each serpentine type are very similar. As usual in natural samples, the structural formulae of serpentines differ slightly from the ideal one. 15 to 20 % of Mg is substituted by Fe which is commonly distributed among the octahedral sites. In this case, the fairly high Fe content for all species can totally compensate for the lack of Mg. Al content is very low (< 0.1 apfu) as previously observed in EMPA. No chemical differences between serpentine types are observed.

5. Interpretation and discussion

5.1. Formation of serpentine banded veins: a crack-seal mechanism

Formation of veins can be split into three steps as follows: 1) crack opening, driven by fluid pressure, stress or crystalliza-

Table 1. Electron microprobe analyses of serpentine.

Analysis	#14	#16	#18	#54	#55	#57	#61	#56	#34	#42	#50
Location	mtx	mtx	mtx	mtx	mtx	CS-15µm	CS-15µm	CS-15µm	CS-45µm	CS-105µm	CS-220µm
Compositions in wt% of oxides											
SiO_2	40.9	40.9	42.8	41.8	41.3	40.3	40.3	40.6	40.1	40.1	40.9
MgO	37.7	38.1	38.6	37.0	37.9	37.5	37.4	37.2	37.2	37.5	36.2
FeO	3.4	3.9	3.6	4.7	4.6	5.0	5.3	5.0	5.3	5.1	5.3
Al_2O_3	0.3	0.4	0.1	0.2	0.2	0.2	0.3	0.3	0.3	0.3	0.3
NiO	0.4	0.2	0.0	0.1	0.1	0.1	0.1	0.1	0.1	0.1	0.1
Cr_2O_3	0.1	0.1	0.0	0.2	0.2	0.2	0.2	0.2	0.2	0.2	0.2
SO_2	0.3	0.2	0.1	0.1	0.1	0.2	0.2	0.2	0.2	0.1	0.1
Cl	0.3	0.3	0.0	0.1	0.1	0.2	0.1	0.2	0.1	0.2	0.2
F	0.0	0.1	0.0	0.1	0.0	0.2	0.0	0.0	0.3	0.1	0.3
Total	83.5	84.5	85.4	84.3	84.5	83.9	83.9	83.8	83.9	83.7	83.5
Stuctural formulae in atom per formula unit (apfu)											
Si	2.01	1.99	2.04	2.04	2.01	1.99	1.99	2.00	1.98	1.98	2.02
Mg	2.76	2.77	2.75	2.68	2.75	2.75	2.75	2.73	2.73	2.76	2.67
Fe	0.14	0.16	0.14	0.19	0.19	0.21	0.22	0.21	0.22	0.21	0.22
Al	0.02	0.02	0.01	0.01	0.01	0.01	0.02	0.02	0.02	0.02	0.02
Ni	0.01	0.01	0.00	0.00	0.00	0.00	0.00	0.00	0.01	0.00	0.00
Cr	0.00	0.00	0.00	0.01	0.01	0.01	0.01	0.01	0.01	0.01	0.01
S	0.01	0.01	0.00	0.00	0.00	0.01	0.01	0.01	0.01	0.00	0.00
Cl	0.02	0.02	0.00	0.00	0.00	0.01	0.01	0.02	0.01	0.02	0.01
F	0.00	0.01	0.00	0.02	0.00	0.02	0.00	0.00	0.05	0.01	0.04
Total	4.98	5.00	4.95	4.96	4.98	5.01	5.00	4.99	5.03	5.01	4.99

Analysis within the matrix: mtx – Analysis within the banded vein: CS-distance to the matrix

Table 2. EDS-TEM microanalyses of serpentine types.

Analysis	#1	#2	#3	#4	#5	#6	#7	#8	#9
Serp. type	proto.s	proto.s	proto.s	ctl	ctl	ctl	polyg.s	polyg.s	polyg.s
Stuctural formulae in atom per formula unit (apfu)									
Si	1.95	1.86	1.90	1.84	2.00	1.95	2.05	1.96	1.79
Mg	2.80	3.02	2.93	2.97	2.59	2.79	2.65	2.80	3.21
Fe	0.24	0.21	0.16	0.24	0.27	0.22	0.22	0.19	0.17
Al	0.02	0.00	0.06	0.06	0.09	0.05	0.02	0.04	0.02
Cr	0.01	0.00	0.00	0.01	0.00	0.01	0.00	0.01	0.00
Ni	0.00	0.00	0.00	0.00	0.01	0.00	0.00	0.00	0.00
Total	5.02	5.10	5.07	5.12	4.95	5.02	4.94	5.01	5.20

Mean value:			
Serp. type	proto.s	ctl	polyg.s
Si	1.91	1.93	1.93
Mg	2.92	2.78	2.89
Fe	0.20	0.24	0.19
Al	0.03	0.07	0.03
Cr	0.00	0.01	0.00
Ni	0.00	0.00	0.00
Total	5.06	5.03	5.05

Proto.s: protoserpentine or P1 phase; ctl: chrysotile or P2 phase; polyg.s: polygonal serpentine or P3 phase.

tion forces; 2) transport of vein forming elements by advection and/or diffusion; 3) crystallization of the vein minerals. Interesting questions concern the origin and preservation of supersaturation within the crack and the capability of internal microstructures to track the displacement history. These points are discussed in the following chapters for the particular case of the serpentine banded vein.

5.1.1. Crack opening and propagation

Banding can have different origins: mineralogical alternances, chemical variations, fluid or rock inclusions... Thus, banding can be formed by different mechanisms. In the studied serpentine banded vein, no chemical variations have been observed across the vein width. SEM images clearly show

that a physical and morphological discontinuity exists between bands. The limit between successive bands is only marked by a discontinuity in the growth of minerals. This suggests that, in this case, banding can be interpreted as a result of individual crack openings, as proposed by the crack-seal process of Ramsay (1980). Oscillations in fluid pressure and/or local stress are usually thought to open the interstice corresponding to each band (Ramsay, 1980). In the particular case of the serpentine banded veins, two possible causes of cracking were proposed, as pointed out in section 2.2: i) incremental stress release due to progressive unroofing of serpentinized blocks (Dilek *et al.*, 1997), or ii) accommodation of volume increase during serpentinization of the peridotite (O'Hanley, 1992). The field evidence and the analytical results are, at this stage, insufficient to discuss this point. Thermal expansion has not been considered since it should not be significant at this range of temperatures (< 500˚C).

The direction of serpentine fibre growth varies in different directions around a preferred orientation. This internal microstructure can only occur in a fluid-filled open-crack where geometrical selection occurs during growth. The preservation of the wall geometry (Fig. 2a) during vein formation is possible only if sealing of a crack is achieved before the opening of the following one. This is consistent with the model proposed by Hilgers *et al.* (2001).

The presence of a poorly crystallized layer at the vein-wall contact (Fig. 3d) from which tubes protrude suggests that addition of a new band occurs at the vein-wall limit, thus defining an antitaxial vein filling. According to the asymetric geometry of the vein tip (Fig. 1c and 1d) and SEM observations, it seems that cracking preferentially occurs at one vein-wall interface and propagates in mode I. The shape of the vein margins is irregular and the morphology of the first crack is preserved during vein formation since each new crack follows the surface of the preceding one (Fig. 1c and 2a). There is no evidence of margin dissolution or cataclastic deformation resulting from crack opening. This has been proposed by Robert & Boullier (1994) to be in favour of a slow or sub-critical propagation mode. Different mechanisms are considered to accommodate such a steady-state mode of propagation (Atkinson, 1984) but too few indices remain in this final deformation state to allow conclusions. Complete filling of the crack by precipitating minerals allows stress transfer through the vein and the opening of another crack at the vein-wall interface. Indeed, the different texture across the vein-host rock interface makes this site a weak area.

5.1.2. Crack filling and capillary effect

When the μm wide crack is opened, it is filled by a fluid to allow mineral precipitation. Then a mass transfer and a localized precipitation in the interstice is needed to explain the vein filling.

Given the very low solubility of phyllosilicates, transport of nutrients by advection through the fracture network would require huge amounts of circulating fluid to fill each interstice totally with minerals, as Fisher & Brantley (1992) already concluded for quartz-filled veins. Furthermore, the interconnectivity between cracks required for fluid circulation and advection is not always observed. There are no significant variations in major elements either within the vein, or between the host rock and vein mineral compositions. This indicates that there is no chemical change in space and time during vein formation, thus suggesting a constant source of matter and no chemical segregation. Others analyses realized on this type of vein confirm that the composition of the vein is sensitive to the composition of the adjacent wall rock (Andreani, 2003). Therefore, the nutrient source may have been the immediately adjacent matrix. Chemical microanalysis shows that vein filling and transformations during the potential protoserpentine-chrysotile-polygonal serpentine sequence occur isochemically. Taken together, these results suggest a closed-system behaviour implying small-scale transport of elements in a fluid by a diffusional process that may have taken place through the walls of the vein thanks to their porosity. A chemical potential gradient due to a pressure, temperature, stress or chemistry gradient is required to establish diffusion and needs to be maintained until total filling of the crack. Supersaturation should also steadily occur in the interstice to allow mineral growth. These points are examined in the following section.

Macroscopic crystal growth theory commonly uses a capillary model based on the analogy between the liquid/vapour and crystal/solute systems (Mullins & Sekerka, 1963). Crystal growth is only possible when it results in a decrease in Gibbs free energy G of the system. Hence the favourable variation of G may be written as:

$$\Delta G = \Delta G_{vol} + \Delta G_{surf} < 0 \qquad (1)$$

where $\Delta G_{vol} = -n.\Delta\mu$ is the volume free energy difference, with n the number of growth (or dissolution) units forming the crystal and having crossed the crystal/medium interface, and $\Delta\mu$ the chemical potential difference undergone by one of those growth units.

$\Delta G_{surf} = +\gamma A$ is the crystal surface contribution to this Gibbs free energy change equal to the product of the crystal surface tension γ (assumed to be isotropic here) multiplied by the crystal surface area A.

Two different cases for nucleation are possible: homogeneous *versus* heterogeneous. In nature, nucleation is predominantly heterogeneous because of the availability of preferential nucleation sites which lower the nucleation activation energy barrier. In this way, the convex nucleus decreases its area in contact with the solution lowering, thereby, the surface energy. This benefit is all the greater if the crystal-chemical affinity between the crystal and support is large. However, ΔG_{surf} remains positive so that we should still have $\Delta G_{vol} < 0$, *i.e.*, $\Delta\mu = kTLn(a/a_{eq}) > 0$ for crystal growth, where k is Boltzman's constant, T the absolute temperature, a the actual solute activity, and a_{eq} the equilibrium activity or solubility at T. Accordingly, crystal growth is only possible if $a/a_{eq} > 1$ that is, if the solution is supersaturated.

Baronnet & Saül (2003) examined theoretically the conditions of crystallization in very tight interstices (around μm and below). They showed that tight interstitial opening favours crystallization in two ways: i) the simultaneous contact of the nucleus with both matrix walls decreases twice

the surface energy for the supported nucleus compared to the free nucleus, ii) good capillary wetting induces a concave crystal/solution meniscus. Effect ii) is important in that it depresses the crystal solubility just as a sub-saturated pressure exists within a liquid in case of capillary condensation. The main point is that surface tension, while pulling the condensed phase, may now act to promote crystallization as $\Delta G_{surf} < 0$ is now possible. In the latter case, $\Delta G < 0$ may be obeyed over a certain range of $\Delta G_{vol} > 0$, or for $\Delta\mu < 0$, *i.e.*, for nominally undersaturated solutions ($a/a_{eq} < 1$). The range of undersaturation concerned increases with the interstice narrowness and with the wetting capability of the crystal/support pair. This situation of possible crystal growth in undersaturated solutions may be seen as analogous, but opposite, to that of Oswald ripening where the capillary effect makes particle dissolution possible in a nominally supersaturated solution.

The driving force for diffusion of the serpentine material from the wall to the crack is related to the difference between the convex grain surface in the matrix and the concave solid/solution meniscus in the interstice. Indeed, the Gibbs-Thomson relationship shows that the solubility of a crystal is inversely proportional to its size. So the activity of the solute in the matrix would be enhanced by the small grain-size of the matrix material (normal capillary effect on solubility), and possibly also by the supersolubility induced by stresses on matrix grains (pressure solution, Weyl, 1959). Contrasting with this, the equilibrium activity inside the vein interstice would be depressed by the above-mentioned reversed solid/solution meniscus effect. The activity gradient responsible for solute diffusion from the matrix to the interstice could result from such physical contrast between the matrix, acting as the solute source, and the vein interstice, acting as the sink. During progressive filling, such activity gradient and diffusional process would even increase owing to the narrower and narrower opening until complete closure. This process depends on the presence of an interstice and should thus stop when the crack is filled. However, its action might be resumed if the seeping capability of the wall for solute inflow were to be refreshed by successive cracks.

Observations show that three different structural types of serpentine coexist in each crack: protoserpentine, chrysotile and polygonal serpentines. Hydrothermal synthesis of serpentines at 300°C and 200°C by Grauby *et al.* (1998), from a stoechiometric (excess H_2O) gel revealed a temporal succession of serpentine types: protoserpentine-chrysotile-polygonal serpentine and much later lizardite (platy structure). This isochemical evolution has been attributed to the decreasing degree of supersaturation of the solution with respect to serpentine. Normand *et al.* (2002) reached the same conclusion for the relative appearance of chrysotile and lizardite. Moreover, it has been suggested that polygonal serpentine, which has a larger diameter than chrysotile, is a more evolved tubular form of serpentine (Baronnet *et al.*, 1994).

Our observations may be indicative for the occurrence of the same succession also in natural samples. A system out of equilibrium would classically favour the precipitation of kinetically controlled (metastable) phases first. The most metastable phase here (the most soluble one) is protoserpentine and should precipitate first in the interstice as soon as it opens and fills with a fluid (Fig. 6, stage 2, Phase P1). Observations and chemical analyses do not support a large-scale fluid circulation, so a variation in serpentine solubility in the interstice can hardly be related to a variation in fluid temperature. A pressure drop linked to a micrometre crack may briefly help nucleation but would not significantly decrease solubility to establish and maintain such a departure from equilibrium. The interstice capillary effect described above would allow the system to diverge considerably from equilibrium as soon as the crack opens, without the need to have a highly supersaturated fluid within the crack. Low surface tension between nucleus and nucleation site, a prerequisite for the model, is expected because precipitated minerals and substrates are both serpentines (high structural and chemical affinity). This preliminary form, protoserpentine, can then evolve into chrysotile tubes with residual porosity due to loss of water by this preliminary "gel-type" serpentine (Fig. 6, stage 3). Chrysotile would preferentially nucleate against the most similar material, *i.e.*, the one it has the most affinity with, and thus against the surface of the crack opposite the vein wall. In this way, the arrival of nutrients from the matrix is not stopped by crack filling and should be able to fill each narrow space completely (Fig. 6, stage 4).

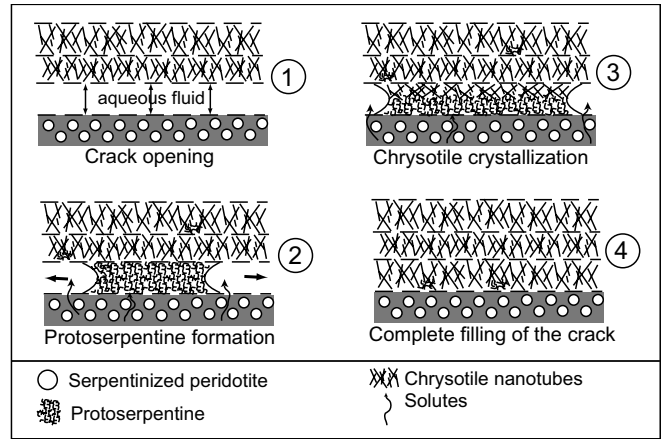

Fig. 6. The different steps of the inferred model of serpentine banded vein formation. It includes four main steps: 1) The µm sized crack opens and is filled with an aqueous fluid. It is accompanied by a small pressure and solubility drop. 2) Protoserpentine (or quasi isotropic gel-type serpentine) forms locally because it is the kinetically favoured metastable phase under such conditions. The crystal forms an inverse solid/solution meniscus with the two walls of the interstice. This depresses the solubility within the crack. The difference between the high activity around the small matrix grains and the lower activity in the interstice creates a diffusional transport of elements that feeds the crack and helps the protoserpentine to propagate laterally. 3) Diffusion can be maintained until total filling of the crack. The chrysotile initially nucleating on the last crack can therefore progressively replace the protoserpentine. Chrysotile can then evolve to a more stable phase, the next one being polygonal serpentine. 4) The crack is filled with a majority of chrysotile and some polygonal serpentines. Some patches of protoserpentine may remain. The diffusional process stops until the system is refreshed by a new crack opening.

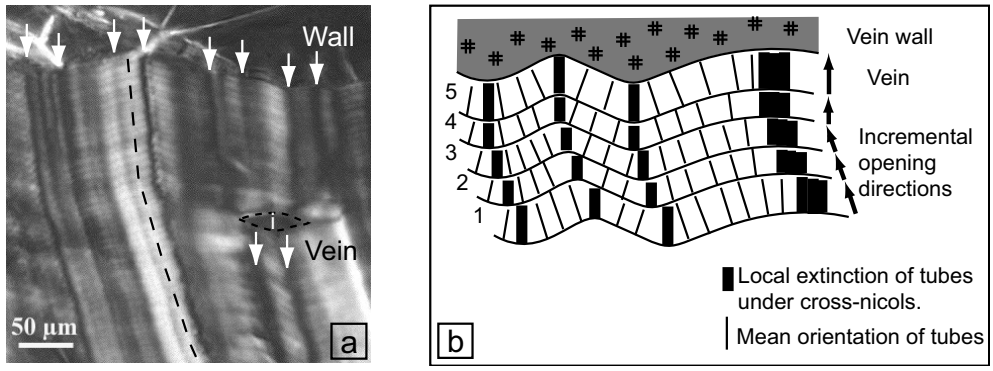

Fig. 7. a: Vein-wall contact under crossed polars. White arrows show margin irregularities. They correspond to the starting points of crystallographic trails parallel to the dotted line across the vein. A wall fragment (i) locally modifies the orientation of the trails. b: Diagram explaining the formation of trails during banded vein formation. The trails are crystallographic since they correspond in each band to the local extinction of the tubes. By following these extinctions, it is possible to join the morphological irregularities of the two walls and to track the opening direction.

Chrysotile grows along the [100] fibre axis and undergoes a progressive geometric segregation leading to the preferred orientation of tubes. Tube zones of higher disorder (Fig. 4a) should therefore appear first and mark the beginning of filling. Growth competition between tubes would then lead to ordered zones (Fig. 4b). If the solute concentration remains high enough, the chrysotile growth, limited by a critical radius of lattice curvature (energy storage constraint), would progressively evolve to polygonal serpentine (Baronnet *et al.*, 1994; Devouard & Baronnet, 1995; Baronnet & Devouard, 1996).

5.2. Origin and efficiency of the tracking capability of the vein opening directions

Syntectonic veins are potential structural markers of strain directions (*e.g.* Durney & Ramsay, 1973; Passchier & Trouw, 1996). Only fibrous and crack-seal veins assumed to form progressively or by opening increments have this potential. The direction of fibre growth or crystal elongation has long been considered to be a direct indication of stretching direction during vein formation. However, it has also been proved that they do not necessarily indicate opening direction (Van Der Pluijm, 1984; Cox, 1987; Williams & Urai, 1989; Urai *et al.*, 1991). These particular internal microstructures have been intensively studied in order to determine the conditions of a real tracking capability. The internal structure of crack-seal veins commonly shows elongate blocky or stretched crystals. The opened crack is assumed to be filled unitaxially (in one direction) by overgrowth of ancient vein crystals exposed to the fluid-filled fracture. The relative influence of different parameters on the tracking capability of antitaxial veins has been investigated through numerical modelling of crystal growth kinetics (Bons, 2001; Hilgers *et al.*, 2001). They lead to the conclusion that opening directions are best recorded by the fibrous crystal long-axis if the fracture is tight, its surface is rough and if it is totally filled before the next opening increment.

In the present crack-seal serpentine veins, fibrous minerals are not distinguishable optically but, under crossed polars, an inhomogeneous extinction across the vein links edge irregularities regardless of banding (Fig. 2a and 2b) as described in part 3.1. The extinction position of serpentine fibres is parallel to their long axis. No deformation has been observed, so banding and extinction are only due to crystallographic orientation during growth. Within one band, fibres are not parallel to each other but they show a preferred orientation that is perpendicular to the limit of the last increment. Extinction occurs when the band limit is parallel to the N-S or E-W axis of the microscope under crossed polars (Fig. 7a) and, therefore, fibre orientation is not displacement-controlled. The separation line between bands is always close to extinction to a certain degree since it represents the limit between the end of a band where the tubes are well oriented (Fig. 4b) and the beginning of a new one marked by remaining protoserpentine patches and disoriented tubes (Fig. 4a) (low birefringence material). Nucleation of the first chrysotile tubes would be easier on the margin of the preceding crack since it is filled with the same serpentine material and some seeds may remain. So the tubes will more probably form perpendicular to the preceding crack than to the wall-rock surface. If the crack surface has asperities, fibre orientation will follow them and the extinction will not occur simultaneously in one band (Fig. 7a and b). Consequently, an oblique opening increment will be recorded by the displacement of the local extinction in the new band. The dotted line in Fig. 2b follows these local extinctions in successive bands across the vein and have a similar signification as inclusion trails (Ramsay, 1980) since they draw the opening vector of the vein. Wall rock inclusions are rare but, when observed, they confirm the displacement paths determined by the crystallographic trails.

6. Conclusions

The characteristics of serpentine banded veins at different scales suggest a crack-seal type process of formation. Vein morphology and chemical analysis favour diffusional transport of nutrients from the adjacent matrix to the vein.

The three different serpentine types observed in each crack: protoserpentine-chrysotile-polygonal serpentine, are described together for the first time in natural samples, and may be compared to the succession described in synthesis experiments during a decreasing supersaturation of an isochemical system.

Based on these observations, we propose a model of formation for serpentine banded veins that could explain: 1) the high departure from the equilibrium required for the precipitation of protoserpentine and 2) the enhancement and the maintaining of a steady-state diffusional process for vein filling. This model takes advantage of capillary effects on crystallization that can occur in micrometre-size interstices. Further observations are needed but this study supports the view that serpentine microstructures may be able to record their environmental growth conditions. Thus they can act as a new tool for understanding crystal growth conditions under dynamic regimes.

Trails, resulting from an inhomogeneous extinction of bands under crossed polars, track the opening direction across the vein. Serpentine banded veins have a very good tracking capability if the surface of the initial fracture is sufficiently rough compared to fibre size.

Development of such veins with discontinuities creates localized weak planes within massive serpentinite blocks that may preferentially accommodate further brittle deformation. This example also shows that, under wet and relatively low temperature conditions, serpentines can accommodate progressive deformation by a dissolution-diffusion-crystallization process. This can also have major implications in other tectonic settings such as the active San Andreas fault, in which serpentinites are abundant especially in seismic creeping segments.

Acknowledgments: We thank C. Nevado, C. Merlet, S. Nitsche and D. Chaudanson for their technical assistance, S.F. Cox and O. Grauby for fruitful discussions, J. Urai and B. Grobéty for their helpful reviews. This work was supported by the Observatoire de Grenoble and the IT02 program of the INSU-CNRS.

References

Andreani, M. (2003): Les microstructures de déformation des serpentines et la partition sismique-asismique: exemple de la Californie. PhD Thesis, Joseph Fourier University, Grenoble, France.

Atkinson, B.K. (1984): Subcritical crack-propagation in geological materials. *J. Geophys. Research*, **89**, 4077-4114.

Atwater, T. (1989): Plate tectonic history of the northeast Pacific and western North America. *in* "The Eastern Pacific Ocean and Hawaii. Geology of North America", E.L. Winterer, D.M. Hussong, R.W. Decker, eds., Geological Society of America, Boulder, Colorado, **N**, 21-71.

Bailey, E.H., Irwin, W.P., Jones, D.L. (1964): Franciscan and related rocks and their significance in the geology of western California. *California Division of Mines and Geology Bull.*, **183**, 177.

Baronnet, A. & Devouard, B. (1996): Topology and crystal growth of natural chrysotile and polygonal serpentine. *J. Crystal Growth*, **166**, 952-960.

Baronnet, A. & Saül, A. (2003): Interstitial crystal growth from undersaturated solutions: a model and geological applications. EGS-AGU-EUG, Nice, Abstract P0308.

Baronnet, A., Mellini, M., Devouard, B. (1994): Sectors in polygonal serpentine. A model based on dislocations. *Phys. Chem. Minerals*, **21**, 330-343.

Bons, P.D. (2001): Development of crystal morphology during unitaxial growth in a progressive widening vein: I. The numerical model. *J. Struct. Geol.*, **23**, 865-872.

Bons, P.D. & Jessell, M.W. (1997): Experimental simulation of the formation of fibrous veins by localised dissolution-precipitation creep. *Min. Mag.*, **61**, 53-63.

Coleman, R.G. (2000): Ultramafic rock (serpentine) in California and Oregon. Standford Geological Survey.

Coleman, R.G. & Keith, T.E. (1971): A chemical study of serpentinization – Burro Mountain, California. *J. Petrol.*, **12**, 311-328.

Cox, S.F. (1987): Antitaxial crack-seal vein microstructures and their relationship to displacement paths. *J. Struct. Geol.*, **9**, 779-787.

Cox, S.F. & Etheridge, M.A. (1983): Crack-seal fibre growth mechanisms and their significance in the development of oriented layer silicate microstructures. *Tectonophysics*, **92**, 147-170.

Devouard, B. & Baronnet, A. (1995): Axial diffraction of curved lattices: geometrical and numerical modeling. Application to chrysotile. *Eur. J. Mineral.*, **7**, 835-846.

Devouard, B., Baronnet, A., Van Tendeloo, G., Amelinckx, S. (1997): First evidence of synthetic polygonal serpentines. *Eur. J. Mineral.*, **9**, 539-546.

Dilek, Y., Coulton, A., Hurst, S.D. (1997): Serpentinization and hydrothermal veining in peridotites at site 920 in the Mark area. *in* "Proceedings of the Ocean Drilling Program, Scientific Results", J.A. Karson, M. Cannat, D.J. Miller, D. Elthon, eds., **153**, 35-59.

Dungan, M.A. (1979): A microprobe study of antigorite and some serpentine polymorphs. *Can. Mineral.*, **17**, 771-784.

Durney, D.W. & Ramsay, J.G. (1973): Incremental strains measured by syntectonic crystal growth. *in* "Gravity and Tectonics", K.A. De Jong & R. Scholten, eds., John Wiley, New York, 67-96.

Ernst, W.G. (1971): Do mineral parageneses reflect unusually high pressure conditions of Franciscan metamorphism? *Am. J. Sci.*, **271**, 81-108.

Fisher, D.M. & Brantley, S.L. (1992): Models of quartz overgrowth and vein formation: deformation and episodic fluid flow in an ancient subduction zone. *J. Geophys. Res.*, **97**, 20043-20061.

Grauby, O., Baronnet, A., Devouard, B., Schoumacker, K., Demirdjian, L. (1998): The chrysotile-polygonal serpentine-lizardite suite synthesized from a $3MgO\text{-}2SiO_2$-excess H_2O gel. The 7th International Symposium on Experimental Mineralogy, Petrology, and Geochemistry, Orléans, Abstracts. *Terra Nova*, supplement **1**, 24.

Hilgers, C., Köhn, D., Bons, P.D., Urai, J.L. (2001): Development of crystal morphology during unitaxial growth in a progressive widening vein: II. Numerical simulations of the evolution of antitaxial fibrous veins. *J. Struct. Geol.*, **23**, 873-885.

Means, W.D. & Li, T. (2001): A laboratory simulation of fibrous veins: some first observations. *J. Struct. Geol.*, **23**, 857-863.

Mullins, W.W. & Sekerka, R.F. (1963): Morphological stability of a particle growing by diffusion or heat flow. *J. Appl. Phys.*, **35**, 323-329.

Normand, C., Williams-Jones, A.E., Martin, R.F., Vali, H. (2002): Hydrothermal alteration of olivine in a flow-through autoclave: nucleation and growth of serpentine phases. *Am. Mineral.*, **87**, 1699-1709.

O'Hanley, D.S. (1992): Solution to the volume problem in serpentinization. *Geology*, **20**, 705-708.

Page, B.M. (1972): Oceanic crust and mantle fragment in subduction complex near San Luis Obispo, California. *Geol. Soc. Amer. Bull.*, **83**, 957-972.

– (1981): The Southern Coast Range. *in* "The geotectonic development of California", G.W. Ernst, ed., Prentice-Hall, Englewood Cliffs, New Jersey, 330-417.

Page, B.M., Thompson, G.A., Coleman, R.G. (1998): Late Cenozoic tectonics of the central and southern Coast Ranges of California. *Geol. Soc. Amer. Bull.*, **110**, 846-876.

Passchier, C. & Trouw, R. (1996). Microtectonics. Springer, Berlin, 289 p.

Ramsay, J.G. (1980): The crack-seal mechanism of rock deformation. *Nature*, **284**, 135-139.

Renard, F., Andreani, M., Boullier, A.M., Labaume, P. (in press): Crack-seal patterns: records of uncorrelated stress release variations in crustal rocks. *in* "Deformation, Mechanisms, Rheology and Tectonics: from Minerals to the Lithosphere", D. Gapais, J.P. Brun, P. Cobbold, eds., Special Publication of the Geological Society of London.

Robert, F. & Boullier, A.M. (1994): Mesothermal gold-quartz veins and earthquakes. *in* "The mechanical involvement of fluids in faulting", S.H. Hickman, R.H. Sibson, R.L. Bruhn, eds., U.S. Geological Survey, Open-file report 94-228, 18-30.

Stamoudi, C. (2002): Processus de serpentinisation des péridotites de Hess-Deep et de la zone de MARK. Approche chimique et minéralogique. PhD Thesis, Paris VI University, France.

Twiss, R.J. & Gefell, M.J. (1990): Curved slicken fibers: a new brittle shear sense indicator with application to a sheared serpentinite. *J. Struct. Geol.*, **12**, 471-481.

Urai, J.L., Williams, P.F., Van Roermund, H.L.M. (1991): Kinematics of crystal growth in syntectonic fibrous veins. *J. Struct. Geol.*, **13**, 823-836.

Van der Pluijm, B.A. (1984): An unusual "crack-seal" vein geometry. *J. Struct. Geol.*, **6**, 593-597.

Viti, C. & Mellini, M. (1998): Mesh textures and bastites in the Elba retrograde serpentinites. *Eur. J. Mineral.*, **10**, 1341-1359.

Weyl, P.K. (1959): Pressure solution and the force of crystallization: a phenomenological theory. *J. Geophys. Research*, **64**, 2001-2025.

Wicks, F.G. & Wittaker, E.J.W. (1977): Serpentine texture and serpentinisation. *Can. Mineral.*, **15**, 459-488.

Williams, P.F. & Urai, J.L. (1989): Curved vein fibres: an alternative explanation. *Tectonophysics*, **158**, 311-333.

Wiltschko, D.V. & Morse, J.W. (2001): Crystallization pressure versus "crack seal" as the mechanism for banded veins. *Geology*, **29**, 79-82.

Zussman, J., Brindley, G.W., Comer, J.J. (1957): Electron diffraction studies of serpentine minerals. *Am. Mineral.*, **42**, 666-670.

Received 16 October 2003
Modified version received 12 February 2004
Accepted 18 March 2004